Stem Cell Reports
Article
ISSCR
OPEN ACCESS

O-GlcNAcase regulates pluripotency states of human embryonic stem cells

Qianyu Liu,[1,7] Cheng Chen,[2,3,7] Zhiya Fan,[4,7] Honghai Song,[5] Yutong Sha,[1] Liyang Yu,[1] Yingjie Wang,[3] Weijie Qin,[4,*] and Wen Yi[1,6,8,*]

[1]Ministry of Education Key Laboratory of Biosystems Homeostasis & Protection, College of Life Sciences, Zhejiang University, Hangzhou 310058, China
[2]Shaoxing People's Hospital, Shaoxing Hospital, Zhejiang University School of Medicine, Shaoxing, Zhejiang 312000, China
[3]State Key Laboratory for Diagnosis and Treatment of Infectious Diseases, National Clinical Research Center for Infectious Diseases, The First Affiliated Hospital, School of Medicine, Zhejiang University, Hangzhou 310003, China
[4]National Center for Protein Sciences Beijing, State Key Laboratory of Proteomics, Beijing Proteome Research Center, Beijing Institute of Lifeomics, Beijing 100026, China
[5]Department of Orthopaedic Surgery, Sir Run Run Shaw Hospital, Zhejiang University School of Medicine, Hangzhou 310058, China
[6]Cancer Center, Zhejiang University, Hangzhou 310058, China
[7]These authors contributed equally
[8]Lead contact
*Correspondence: aunp_dna@126.com (W.Q.), wyi@zju.edu.cn (W.Y.)
https://doi.org/10.1016/j.stemcr.2024.05.009

SUMMARY

Understanding the regulation of human embryonic stem cells (hESCs) pluripotency is critical to advance the field of developmental biology and regenerative medicine. Despite the recent progress, molecular events regulating hESC pluripotency, especially the transition between naive and primed states, still remain unclear. Here we show that naive hESCs display lower levels of *O*-linked *N*-acetylglucosamine (*O*-GlcNAcylation) than primed hESCs. *O*-GlcNAcase (OGA), the key enzyme catalyzing the removal of O-GlcNAc from proteins, is highly expressed in naive hESCs and is important for naive pluripotency. Depletion of OGA accelerates naive-to-primed pluripotency transition. OGA is transcriptionally regulated by EP300 and acts as a transcription regulator of genes important for maintaining naive pluripotency. Moreover, we profile protein *O*-GlcNAcylation of the two pluripotency states by quantitative proteomics. Together, this study identifies OGA as an important factor of naive pluripotency in hESCs and suggests that *O*-GlcNAcylation has a broad effect on hESCs homeostasis.

INTRODUCTION

Pluripotency is a fundamental feature of embryonic stem cells (ESCs) that give rise to all cell types in an organism. It is accepted that human ESCs (hESCs) possess two distinct states of pluripotency, naive and primed states (Guo et al., 2016; Theunissen et al., 2014). Naive hESCs resemble pre-implantation epiblasts and display the highest developmental potential. Primed hESCs are developmentally more advanced than the naive cells and resemble post-implantation epiblasts (Guo et al., 2016; Van der Jeught et al., 2015). ESCs in these two states are different in various ways, including morphology, clonogenicity, signaling pathways, epigenetic features, and metabolism (Bao et al., 2009; Guo et al., 2016; Nichols and Smith, 2009; Sperber et al., 2015; Van der Jeught et al., 2015). The hESCs cultured in conventional conditions are in the primed state (Nichols and Smith, 2009; Van der Jeught et al., 2015). It is appealing to convert primed hESCs back to the naive state, as naive hESCs are unique to study early embryogenesis and lineage decisions. Although several methods have been developed to convert primed hESCs to naive hESCs (Bayerl et al., 2021; Bredenkamp et al., 2019; Takashima et al., 2014), our current understanding of mechanisms underlying their transition still remains in its infancy.

O-GlcNAcylation is a prevalent form of protein glycosylation that modifies serine and/or threonine residues of intracellular proteins (Hart et al., 2007). *O*-GlcNAc transferase (OGT) catalyzes the addition of *O*-GlcNAc onto proteins, while *O*-GlcNAcase (OGA) hydrolyzes *O*-GlcNAc from proteins (Hanover et al., 2010; Yang and Qian, 2017). Increasing evidence suggests that *O*-GlcNAc plays critical roles in maintaining cell homeostasis through various mechanisms, including transcriptional and epigenetic regulation, signal transduction, metabolic reprogramming, and stress response (Hardivillé and Hart, 2014; Singh et al., 2015; Yang and Qian, 2017). Recently, *O*-GlcNAc has emerged as a key regulator of stem cell identity and cell fate decision. For example, *OGT* deletion in mouse, zebrafish, or frog leads to developmental defects, or even embryonic lethality (Love et al., 2010; Shafi et al., 2000). *OGA* deletion leads to perinatal lethality or developmental delay (Keembiyehetty et al., 2015; Yang et al., 2012). *O*-GlcNAc regulates ESCs self-renewal and pluripotency by controlling the stability and transcriptional activity of key transcription factors, including OCT4, SOX2, ESRRB, and SP1 (Constable et al., 2017; Hao et al., 2019; Lee et al., 2016; Myers et al., 2016). OGT also interacts with and modifies ten-eleven translocation family proteins and other epigenetic cofactors, including HCF1, to regulate ESC differentiation (Deplus et al., 2013; Maury et al., 2015; Vella et al., 2013). Our previous study demonstrated that *O*-GlcNAc regulates the methionine cycle to impact mouse ESC (mESC) pluripotency (Zhu et al., 2020). These studies

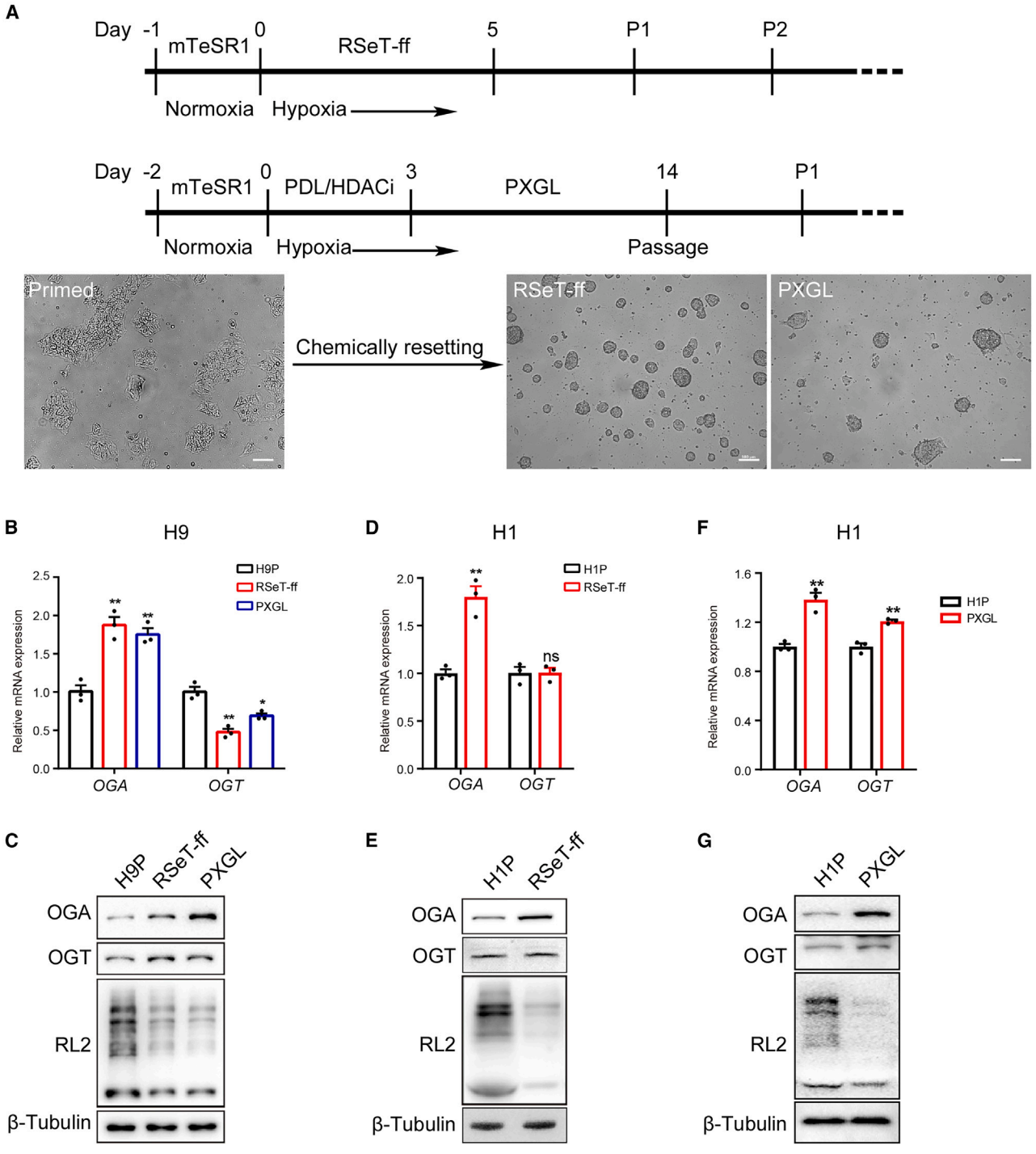

Figure 1. OGA expression is increased in naive hESCs compared to primed hESCs

(A) Schemes and representative pictures for inducing primed hESCs into naive hESCs via RseT-ff and PXGL culture systems. Scale bars, 100 μm.

(B) qPCR analysis of OGA and OGT in H9 primed versus naive hESCs (n = 3 independent assays).

(C) Western blot analysis of OGA, OGT, and O-GlcNAcylation levels (RL2) in H9 primed versus naive hESCs (n = 3 independent assays).

(D) qPCR analysis of OGA and OGT in H1 primed versus RSeT-ff naive hESCs (n = 3 independent assays).

(E) Western blot analysis of OGA, OGT, and RL2 levels in H1 primed versus RSeT-ff naive hESCs (n = 3 independent assays).

(legend continued on next page)

on the function and mechanism of *O*-GlcNAc in ESCs were mainly carried out using mESCs. It is known that mESCs and hESCs differ substantially in various ways (Tsogtbaatar et al., 2020; Varzideh et al., 2023). The role of *O*-GlcNAc and the recycling enzymes (OGT and OGA) in hESCs homeostasis remains largely unexplored.

Here, we sought to delineate the role of OGA in the maintainance and transition of the two states of hESCs. We show that OGA expression is upregulated in naive hESCs and is important for naive pluripotency. In contrast, OGA inhibition has no effect on the primed pluripotency. OGA depletion accelerates the naive-to-primed transition, while OGA expression promotes the primed-to-naive transition. Our results indicate that OGA acts as a transcription regulator of genes important for maintaining naive pluripotency in hESCs.

RESULTS

OGA expression is increased in naive hESCs compared to primed hESCs

To reprogram primed hESCs to the naive state, we induced two primed hESCs lines, H1 and H9, via either the feeder-free (RSeT™ Feeder- Free Medium, RSeT-ff) system or the feeder-dependent (PXGL medium) system (Figure 1A), both of which have been well established (Bredenkamp et al., 2019; Ward et al., 2017). Consistent with previous studies (Collier and Rugg-Gunn, 2018; Taei et al., 2020), the change of colony morphology (Figure 1A), upregulation of naive markers (Figures S1A and S1D), and enhanced single-cell clonogenicity indicate the successful acquisition of naive-like hESCs (Figure S1B). Cells induced with the RSeT-ff system showed lower upregulation of naive markers compared to the PXGL system, consistent with the previous study (Chen et al., 2024). Western blot detected a higher level of the naive marker KLF4 in reprogrammed hESCs than in primed cells (Figure S1C). In addition, in the PXGL system, reprogrammed hESCs displayed characteristic SUSD2^{+}/CD24^{-} cell surface markers distinguished from primed cells with SUSD2^{-}/CD24^{+} markers (Figure S1E). Together, we successfully reprogrammed primed hESCs to naive hESCs.

Next, we examined levels of OGA, OGT, and *O*-GlcNAc in both primed and naive hESCs. Notably, both mRNA and protein levels of OGA increased significantly in H9 and H1 naive cells compared to the primed cells (Figures 1B–1G). Accordingly, *O*-GlcNAc levels were decreased in naive hESCs (Figures 1C–1E, G). In contrast, OGT levels did not show consistent changes (Figures 1B–1G). Our recent proteomic study of naive and primed hESCs showed that OGA was among the top 20 upregulated proteins in naive cells (Figures S1F and S1G). Thus, naive hESCs possess a higher level of OGA and a lower level of *O*-GlcNAc compared to primed cells.

OGA regulates naive pluripotency of hESCs

To investigate the role of OGA in pluripotency and proliferation of naive hESCs, we depleted OGA in naive H9 cells induced via both systems, which caused a drastic reduction of NANOG and SOX2 protein levels (Figures 2A and 2B). A range of naive markers were also significantly reduced (Figures 2C and 2D). Moreover, OGA depletion reduced positive clone ratio for alkaline phosphatase (AP) staining and changed the typical dome-shaped morphology to the flat morphology (Figures 2E and 2F). In contrast, lineage-specific genes were significantly increased (Figures 2G and 2H). These results suggest the impaired pluripotency and naive identity upon OGA depletion in naive hESCs. To further investigate whether OGA activity is required for the naive pluripotency, we treated naive H9 cells with a selective OGA inhibitor thiametG (TMG). TMG treatment similarly decreased the expression of pluripotency markers and naive markers (Figures 2I–2L), reduced the AP-positive colonies (Figures 2M and 2N), and increased the expression of lineage-specific genes (Figures 2O and 2P). We corroborated the aforementioned results using naive H1 hESCs. Consistently, we observed that OGA depletion or inhibition similarly reduced expressions of pluripotent markers and naive markers, as well as positive clone numbers of AP staining (Figures S2A–S2G). To further support the importance of OGA activity in naive pluripotency, we introduced the catalytically dead OGA mutant (K98A) into OGA-depleted naive cells. The results showed that, introduction of wild-type (WT), but not K98A, OGA could effectively restore naive pluripotency (Figures S2L and S2M). Together, these data demonstrate that OGA is important for naive pluripotency of hESCs.

We next investigated the role of OGA in the proliferation of naive hESCs. OGA depletion did not have any appreciable effect on colony formation or cell proliferation rate of naive H9 cells (Figures S2H–S2K), suggesting that OGA is not required for proliferation of naive hESCs.

As OGT catalyzes the opposing reaction compared to OGA, we examined whether modulation of OGT has any effects on naive hESCs. Naive hESCs treated with OSMI-4, a selective OGT inhibitor, reduced global *O*-GlcNAc levels but

(F) qPCR analysis of OGA and OGT in H1 primed versus PXGL naive hESCs ($n = 3$ independent assays).
(G) Western blot analysis of OGA, OGT, and RL2 levels in H1 primed versus PXGL naive hESCs ($n = 3$ independent assays). Error bar represents means ± SEM. ns, nonsignificant, $*p < 0.05$, $**p < 0.01$ (unpaired Student's t test).

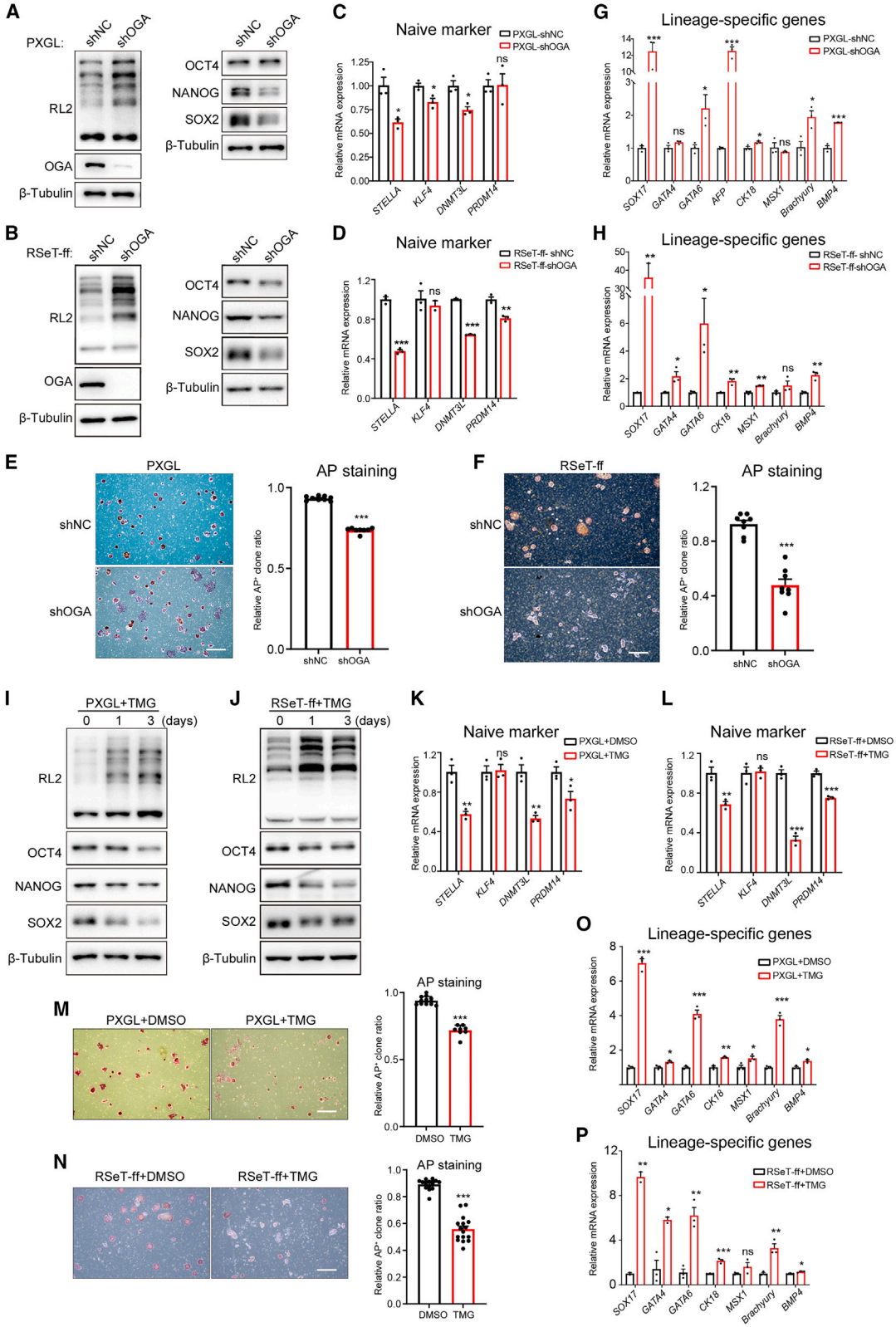

(legend on next page)

slightly increased the expression of SOX2 (Figures S3A, S3B, S3F, and S3G) and naive markers *STELLA* and *PRDM14* (Figure S3C). Consistently, no significant difference was observed for positive clone ratio of AP staining in the presence or absence of OSMI-4, but it was observed that OGT inhibition resulted in smaller clonal morphology of naive hESCs, which suggests a proliferation defect (Figures S3D and S3E). We speculate that these results may be due to the fact that naive hESCs are already in a high pluripotency state. These data suggest that OGT activity is not required for naive pluripotency.

OGA inhibition has no effect on pluripotency of primed hESCs

We then investigated the role of OGA in primed hESCs. Inhibition of OGA with TMG had no effects on the expression of pluripotent markers OCT4, NANOG, and SOX2 in H9 primed cells (Figures S4A and S4B). Consistently, no difference was observed in AP-positive staining compared to the control (Figure S4C). Similar results were obtained with H1 primed cells (Figure S4D). Together, it suggests that OGA inhibition has no effect on pluripotency of primed hESCs.

We further treated H9 primed cells with OSMI-4 and observed a significant reduction of pluripotency markers (Figures S4B, S4E, S4F), AP-positive staining (Figure S4C), and primed markers (Figure S4G). In line with the reduction of pluripotency, the expression of lineage-specific genes was increased upon OGT inhibition (Figure S4H). These data show that OGT inhibition impairs pluripotency of primed hESCs.

OGA affects transitions between naive and primed states

We next investigated whether OGA modulation influences the transition of hESCs between naive and primed states. As naive hESCs possess a higher level of OGA compared to primed hESCs, we knocked down OGA in naive cells and then induced naive-to-primed transition (a process referred to as "repriming") (Figure 3A) (Huang et al., 2021). Analysis of the mRNA levels of primed markers showed a more rapid induction in OGA-depleted cells compared to the control (Figures 3B and 3C). On day 7 of repriming, the percentage of $SUSD2^{-}CD24^{+}$ primed cells reached 50.66% in OGA-depleted cells, compared to 40.76% in control cells in the PXGL system (Figure 3D). These results indicate that OGA depletion accelerates naive-to-primed transition of hESCs.

On the other hand, we ectopically expressed OGA in primed hESCs and reprogrammed cells back to the naive state. Notably, the mRNA levels of naive markers (*STELLA*, *DNM3TL*, and *DPPA5*) were induced more rapidly during reprogramming in OGA-expressed cells than in control cells (Figure 3E), suggesting that OGA expression promotes primed-to-naive transition of hESCs.

EP300 upregulates OGA transcription in naive hESCs

As OGA transcription was upregulated in naive hESCs, we sought to identify the potential transcription factor(s) or cofactor(s) regulating OGA expression. The promoter region of OGA was defined as about 1,500 bp upstream of the transcription start site (TSS) and 200 bp downstream of TSS. The putative promoter was provided to the University of California Santa Cruz (UCSC) Genome Browser (https://genome.ucsc.edu) (Figure 4A). A total of 192 transcription factors were obtained. Alternatively, we predicted possible transcription factors of OGA using hTFtarget, and 184 transcription factors were obtained. There are 76 transcription factors predicted by both datasets. Then we chose six stem cell-associated transcription factors or cofactors for further verification, which include STAT3, ETS1, c-MYC, HIF1a, JUN, and EP300 (Figure 4A). Among them, depletion of *STAT3*, *c-MYC*, *JUN*, and *EP300* resulted in a reduction of *OGA* mRNA levels (Figure S5A). However, c-MYC protein level was upregulated in H9 primed cells and downregulated in naive cells, opposite to the trend of OGA expression (Figure 4B). Thus, we narrowed down the list to STAT3, JUN, and EP300. We then examined the effect

Figure 2. OGA has a role in regulating pluripotency of naive hESCs

(A and B) Western blot analysis of OGA, RL2, and pluripotent markers in H9 naive hESCs upon OGA depletion ($n = 3$ independent assays).
(C and D) qPCR analysis of naive markers in H9 naive hESCs upon OGA depletion ($n = 3$ independent assays).
(E and F) Representative images of AP staining and statistical graph of AP-positive clones ratio in H9 naive hESCs infected with scramble or OGA-targeting short hairpin RNA (shRNA) ($n = 3$ independent assays). Scale bars, 200 μm. The quantification was performed using ImageJ.
(G and H) qPCR analysis of the lineage-specific genes in H9 naive hESCs upon OGA depletion ($n = 3$ independent assays).
(I and J) Western blot analysis of RL2 levels and pluripotent markers in H9 naive hESCs treated with TMG for different time points ($n = 3$ independent assays).
(K and L) qPCR analysis of naive markers in H9 naive hESCs with TMG treatment ($n = 3$ independent assays).
(M and N) Representative images of AP staining and statistical graph of AP-positive clones ratio in H9 naive hESCs with TMG treatment ($n = 3$ independent assays). Counting was performed using ImageJ.
(O and P) qPCR analysis of the lineage-specific genes in H9 naive hESCs with TMG treatment ($n = 3$ independent assays). Error bar represents means ± SEM. ns, nonsignificant, $*p < 0.05$, $**p < 0.01$, $***p < 0.001$ (unpaired Student's t test).

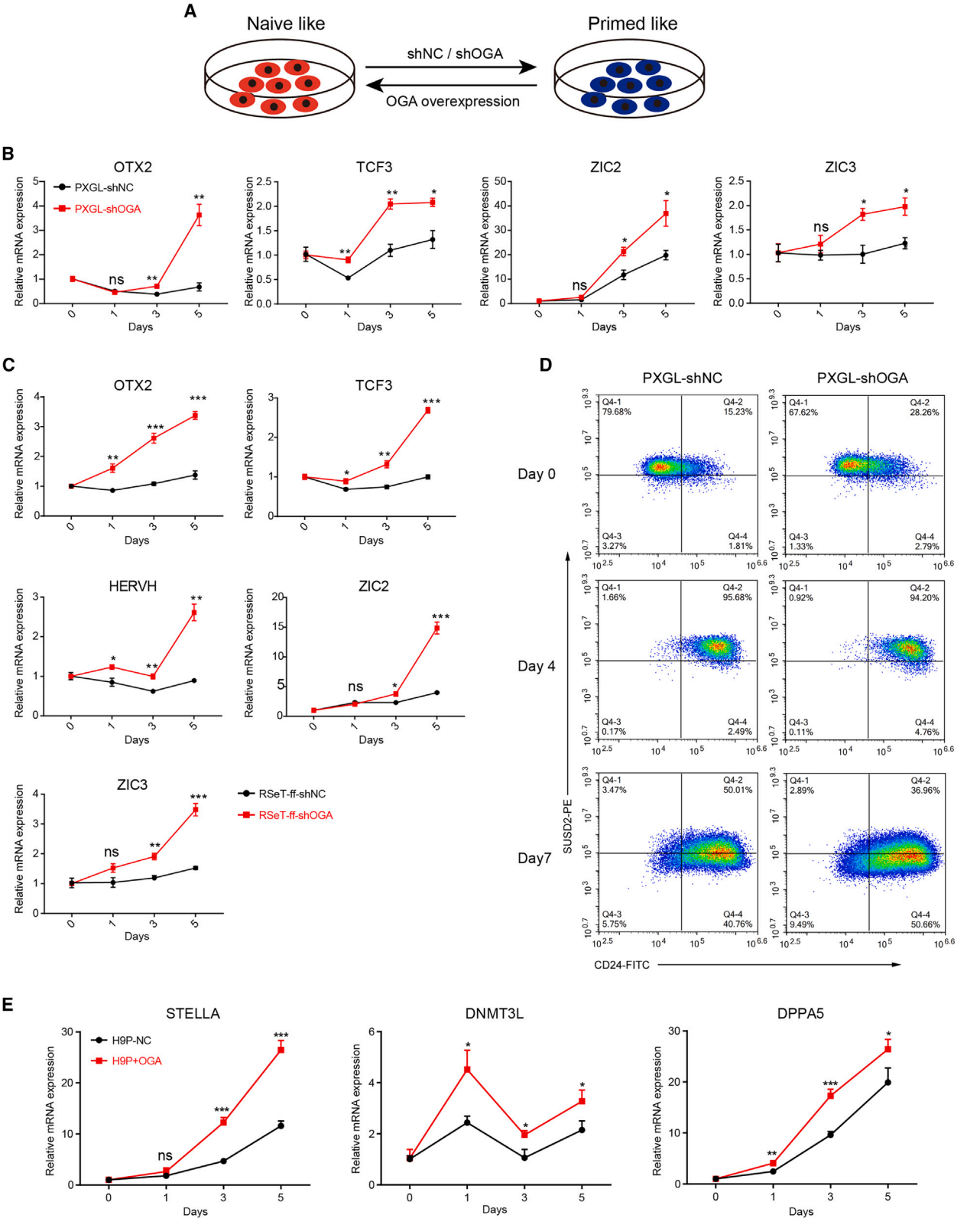

(legend on next page)

on naive pluripotency upon depletion of the three proteins. Notably, pluripotency was significantly decreased only upon *EP300* depletion (Figure 4C), which had a similar phenotype as with OGA depletion. Moreover, EP300 depletion reduced OGA expression and increased global O-GlcNAc levels in naive hESCs (Figure 4D). We further performed dual luciferase reporter assays and observed that EP300 could bind to the promotor region and transactivate OGA (Figure 4E). On the other hand, the reduced expression of OCT4 and NANOG upon EP300 depletion was partially recovered by forced expression of OGA (Figures 4F and 4G). In addition, we performed RNA sequencing (RNA-seq) in PXGL naive hESCs depleted of OGA, depleted of EP300, or depleted of EP300 with OGA re-expression. There were 770 differentially expressed genes (DEGs) co-upregulated in OGA-depleted and EP300-depleted hESCs; among them 357 genes were restored upon OGA re-expression. Among the co-downregulated 433 DEGs, 35 genes were restored (Table S1). Enrichment analysis of restored genes revealed that OGA can rescue EP300-depleted phenotypes associated with extracellular matrix (ECM), embryonic development, and differentiation (Figure 4H). Together, these results suggest that EP300 transcriptionally regulates OGA to impact naive pluripotency.

To investigate the mechanism by which EP300 regulates *OGA* transcription, we tested whether EP300 directly binds to *OGA* promoters. We designed 8 pairs of primers that cover the entire predicted *OGA* promoter region (Figure S5B) and performed chromatin immunoprecipitation-quantitative PCR (ChIP-qPCR) assays. Significant enrichment of EP300 was observed with all 8 pairs of primers, with primer 3, 4, and 5 being the highest in either H9 or H1 primed hESCs (Figures S5C and S5D). Interestingly, EP300 ChIP sequencing (ChIP-seq) data of H1 primed hESCs derived from the Encyclopedia of DNA Elements (ENCODE) database showed a binding peak of EP300 at the *OGA* promoter (Figure S5E). Furthermore, we conducted an EP300 ChIP-seq assay in PXGL naive hESCs, which showed a notable binding peak of EP300 at the *OGA* promoter (Figure 4I). Inspection of genome-wide peak distribution revealed that EP300 binding sites were mainly located at the promoters, introns, and distal intergenic regions (Figure S5F). The Hypergeometric Optimization of Motif EnRichment (HOMER) motif analysis for EP300 binding peaks indicated that EP300 may target transcription factors (e.g., NANOG, KLF5, TEAD1) known to be involved in gene transcription and embryonic organ development (Figure S5G). In addition, EP300-regulated genes are mainly involved in protein modification, metabolism, and gene transcription (Figure S5H). Besides, ChIP-qPCR assays were performed to further verify the significant enrichment of EP300 at the primer3, 4, and 5 regions of the *OGA* promoter (Figures 4J and 4K).

Considering the histone acetyltransferase activity of EP300, we next examined the acetylation states of histones at the *OGA* promoter region in naive hESCs. It is known that histone H3 lysine 9 (H3K9), lysine 14 (H3K14), and lysine 27 (H3K27) residues are substrates of EP300, and their acetylation usually leads to transcriptional activation of downstream genes (McManus and Hendzel, 2003). ChIP-qPCR assays were performed with specific antibodies against acetyl-H3K9, acetyl-H3K14, and acetyl-H3K27, respectively. The result showed that the signal of acetyl-H3K14 at the primer 3 and 4 binding regions decreased significantly upon EP300 depletion in naive hESCs compared with the control, as well as acetyl-H3K27 at the primer 3, 4, and 5 binding regions (Figure 4L). In contrast, no significant difference was observed for the signal of acetyl-H3K9, suggesting that EP300 regulates H3K14 and H3K27 acetylation but not H3K9 acetylation at the *OGA* promoter region. Together, our data indicate that transcriptional regulation of *OGA* by EP300 may be mediated through histone acetylation at the *OGA* promoter region in naive hESCs.

OGA depletion impacts global gene expressions to regulate pluripotency of hESCs

To gain a better understanding of how OGA regulates hESCs pluripotency, we performed RNA-seq analysis to compare gene expressions during PXGL naive-to-primed transition (Figure 5A). There were 2,809 and 6,382 DEGs significantly upregulated in WT PXGL naive and reprimed

Figure 3. OGA modulation affects transition between naive and primed states

(A) Schematic depiction of promoting transitions between naive and primed states.

(B) qPCR analysis of primed markers at different time points during transition from PXGL naive to primed state in hESCs infected with scramble or OGA-targeting shRNA (n = 3 independent assays).

(C) qPCR analysis of primed markers at different time points during transition from RseT-ff-naive to primed state in hESCs infected with scramble or OGA-targeting shRNA (n = 3 independent assays).

(D) Flow cytometry analysis of SUSD2 and CD24 expressions during transition from PXGL naive to primed state in hESCs infected with scramble or OGA-targeting shRNA (n = 3 independent assays).

(E) qPCR analysis of naive markers at different time points during transition from primed to naive state in hESCs with or without OGA overexpression (n = 3 independent assays). Error bar represents means ± SEM. ns, nonsignificant, *p < 0.05, **p < 0.01, ***p < 0.001 (unpaired Student's t test).

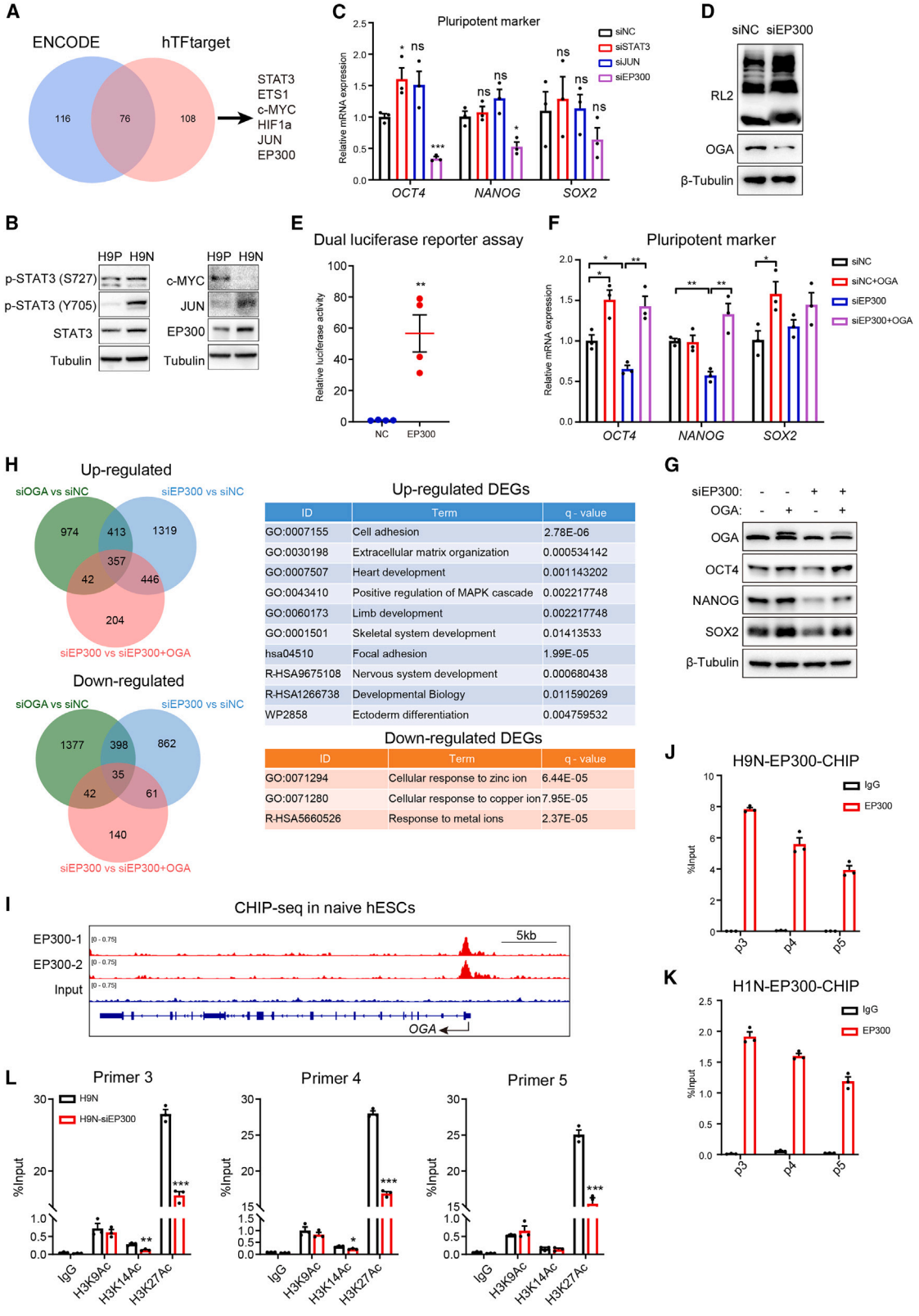

(legend on next page)

H9 hESCs, respectively (Figure 5B; Table S2). Clustering analysis of DEGs indicates that repriming cells possessed intermediate transcriptional identity (Figure 5C). During 5 days of repriming, 3,332 (out of 6,382, 52%) and 1,183 (out of 2,809, 42%) DEGs were significantly up- and downregulated, respectively, compared with naive WT hESCs (Figure S6A). Consistent with the role of OGA in naive pluripotency, OGA depletion caused a significant reduction of naive-related gene expressions, but a significant increase of primed-related gene expressions in naive hESCs (Figures S6B and S6C). Gene set enrichment analysis (GSEA) of naive hESCs showed that cell differentiation pathways and fibroblast growth factor (FGF)/mitogen-activated protein kinase (MAPK) signaling pathways that were usually inhibited in naive hESCs were upregulated upon OGA depletion, as well as ECM-related pathways that participate in embryonic development (Eastham et al., 2007). In contrast, pathways related to oxidative phosphorylation, which usually displays a higher level in naive hESCs (Zhou et al., 2012), were downregulated (Figure 5D). On day 5, 222 DEGs were upregulated and 200 DEGs were downregulated in OGA-depleted cells compared with the WT hESCs (Figure 5E). Consistent with promoting naive-to-primed transition upon OGA depletion, upregulated DEGs include cell differentiation-related genes such as *GATA4* and *TBXT* and primed-specific genes *OTX2*, *CER1*, and *DUSP6*.

We further analyzed the DEGs shared by all three stages upon OGA depletion (Figures 5F and 5G). *MMP2*, participating in epithelial-mesenchymal transition (EMT) during embryonic development (Eastham et al., 2007), was upregulated among the three stages. The lineage-determining transcription factor *GATA6*, which promotes the inner cell mass (ICM) commitment to the primitive endoderm (PrE) (Thompson et al., 2022), was also upregulated. We further differentiated naive hESCs into PrE and nEND (Linneberg-Agerholm et al., 2019) and observed a significant increase in the expression of PrE markers in either PrE or naïve extra-embryonic endoderm (nEND) cells upon OGA depletion (Figure S6D), suggesting that depletion of OGA accelerated the differentiation of naive hESCs toward PrE. *FBXO15*, a target of OCT3/4 and SOX2 (Donato et al., 2017), which was associated with the entrance of primed pluripotency, was significantly downregulated (Figure 5G). GSEA analysis between WT and OGA-depleted cells in the three stages showed an enrichment of two major cellular pathways: cell differentiation/embryonic development and transcription regulation (Figure 5H). These data further support the role of OGA in maintaining naive pluripotency.

Next, we focused on the DEGs affected by OGA depletion during naive-to-primed transition by comparing the DEGs between the naive and repriming stages (Figure 5I). There were 4,187 and 3,933 DEGs upregulated in WT and OGA-depleted hESCs, respectively. Among them 2,884 genes were shared. Among the downregulated DEGs 1,083 genes were shared. Enrichment analysis of these common DEGs showed that upregulated genes were enriched in ECM-related pathways and MAPK pathways, while

Figure 4. EP300 upregulates OGA transcription in naive hESCs

(A) Venn diagram of potential transcription factors that bind to the OGA promoter between the UCSC-ENCODE database and hTFtarget database, as well as transcription factors chosen for downstream research.

(B) Western blot analysis of the expression level of STAT3, c-MYC, JUN, and EP300 in H9 primed and naive hESCs (n = 3 independent assays).

(C) qPCR analysis of pluripotency markers in H9 naive hESCs upon depletion of STAT3, JUN, and EP300 (n = 3 independent assays).

(D) Western blot analysis of OGA and RL2 levels in H9 naive hESCs upon EP300 depletion (n = 3 independent assays).

(E) Dual luciferase reporter assay was performed to test the transcriptional activation ability of EP300 on OGA promotor (n = 4 independent assays).

(F) qPCR analysis of OCT, NANOG, and SOX2 in H9 naive hESCs upon EP300 depletion and ectopic expression of OGA. (n = 3 independent assays).

(G) Western blot analysis of OGA and pluripotent markers in H9 naive hESCs upon EP300 depletion and ectopic expression of OGA (n = 3 independent assays).

(H) Left, Venn diagram showing the overlap of up- or downregulated DEGs between siOGA versus siNC, siEP300 versus siNC, and siEP300 versus siEP300+OGA group. Right, enrichment analysis of the common upregulated or downregulated genes in the three comparison groups.

(I) Integrative genomics viewer images showing tracks of EP300 occupancy on OGA in PXGL naive hESCs.

(J) The binding of EP300 to the primer 3, 4, and 5 regions of OGA is analyzed by ChIP-qPCR in H9 naive hESCs. ChIP-qPCR data were normalized to input. IgG served as a negative control (n = 3 independent assays).

(K) The binding of EP300 to the primer 3, 4, and 5 regions of OGA is analyzed by ChIP-qPCR in H1 naive hESCs. ChIP-qPCR data were normalized to input. IgG served as a negative control (n = 3 independent assays).

(L) The acetylation state of H3K9, H3K14, and H3K27 on the promoter region of OGA is analyzed by ChIP-qPCR using P3, P4, and P5 primers in H9 naive hESCs upon EP300 depletion (n = 3 independent assays). Error bar represents means ± SEM. ns, nonsignificant, $*p < 0.05$, $**p < 0.01$, $***p < 0.001$ (unpaired Student's t test).

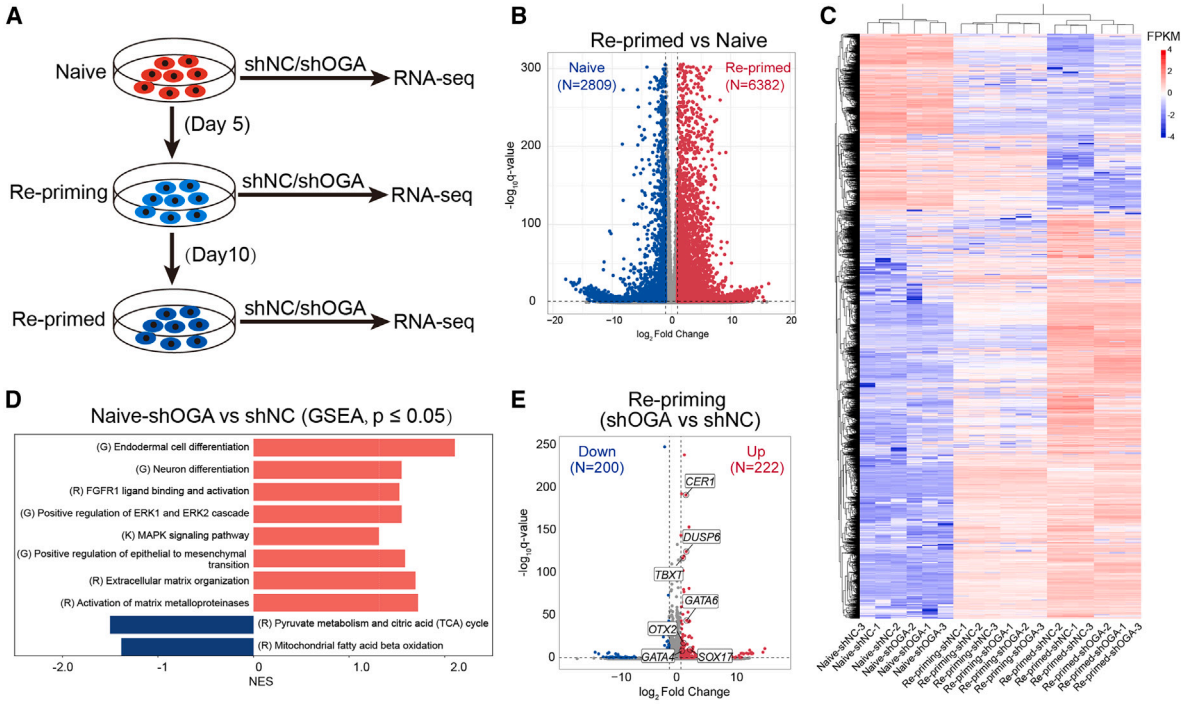

F

shOGA vs shNC

	Genes up	Genes down
Naive	541	320
Re-priming	222	200
Re-primed	1144	815

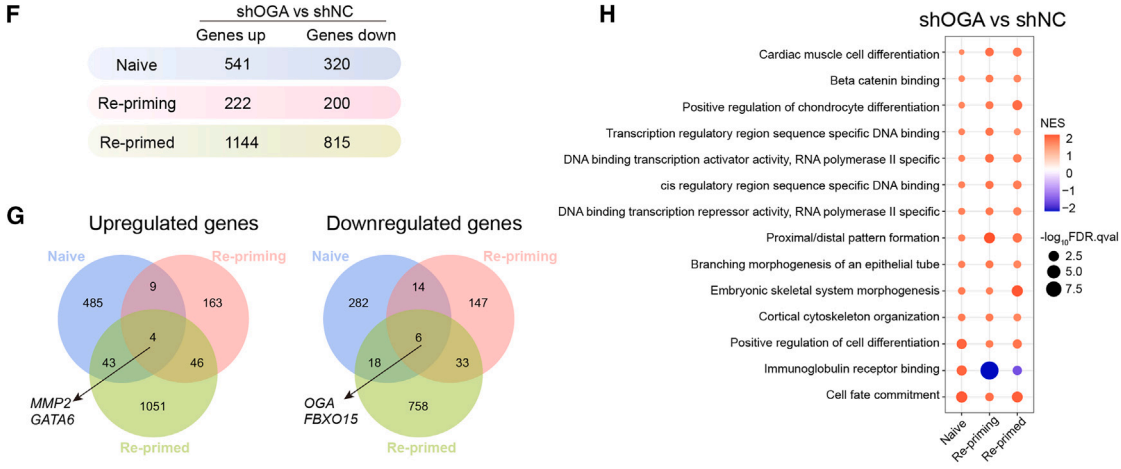

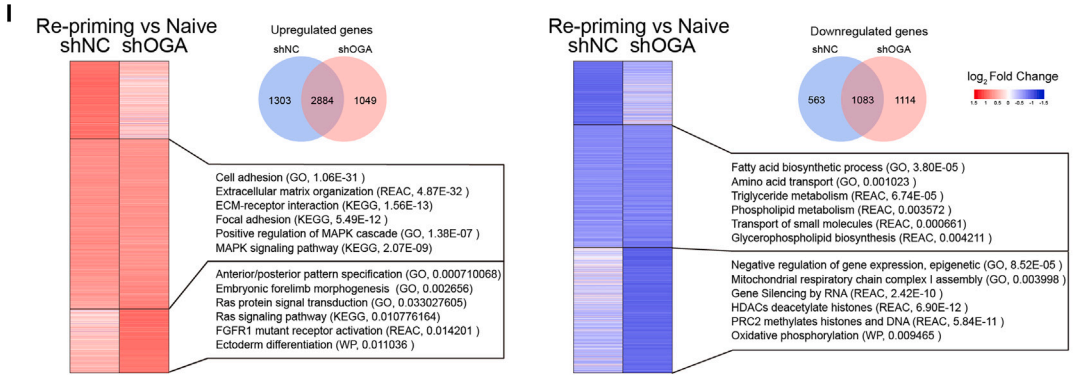

(legend on next page)

downregulated genes were enriched in lipid metabolic and small molecule transport pathways. Further analysis of upregulated (1,049) and downregulated (1,114) genes specifically in OGA-depleted cells showed that FGF/MAPK pathways and differentiation-related pathways were upregulated, while mitochondrial respiration and epigenetic-related pathways were downregulated. These analyses suggest that OGA depletion promotes naive-to-primed transition by upregulating differentiation-related pathways and FGF/MAPK pathways and downregulating oxidative respiration and epigenetic-related pathways.

OGA is involved in transcriptional regulation of pluripotency-related genes in hESCs

Considering its broad impact on gene expression, we subjected PXGL naive hESCs to Cleavage Under Targets & Tagmentation (CUT&Tag) assays. Enrichment for occupancy by OGA was probed with a specific antibody against OGA in WT or OGA-depleted PXGL naive hESCs. Control experiments were carried out with immunoglobulin G (IgG). There were 8,978 peaks overlapped in WT PXGL naive cells. Expectedly, in OGA-depleted cells reads around the center of OGA binding were significantly decreased compared to WT cells (Figure 6A). Inspection of genome-wide peak distribution revealed that OGA binding sites were mainly located at the promoter, introns, and distal intergenic regions (Figure 6B). To identify relevant genes directly regulated by OGA, we integrated the CUT&Tag data with the RNA-seq datasets according to the flowchart shown in Figure 6C. We observed that 4,952 genes contained OGA binding sites, suggesting that these genes maybe directly regulated by OGA. The significant difference analysis revealed 117 DEGs (Table S3). These OGA-targeted DEGs include genes involved in MAPK/ERK signaling, cell differentiation, and ECM-related pathways, which were upregulated upon OGA depletion (Figures 6D and F), as well as genes involved in signal transduction and pluripotency, which were downregulated (Figure 6E). Interestingly, we observed that among the DEGs were 13 genes (all upregulated upon OGA depletion) that encode distinct histone variants (Figure 6F), which were recently emerging as important regulators of ESC identity and cell fate (Li et al., 2022; Pan and Fan, 2016). Further, the HOMER motif analysis for OGA binding peaks of 117 DEGs suggests that OGA may target transcription factors (e.g., FOXA1, NeuroG2, SOX9) known to involve in stem cell differentiation (Figure 6G). Interestingly, it was observed that OGA binds to the promoter region of naive markers *STELLA*, *DNMT3L*, and *PRDM14*, suggesting that OGA may directly regulate naive gene expressions (Figure 6H). Together, these results suggest that OGA is involved in the transcriptional regulation of genes important for the maintenance of naive pluripotency in a *trans*-acting fashion.

Profiling OGA-mediated protein O-GlcNAcylation of the two pluripotency states

As OGA catalyzes hydrolysis of *O*-GlcNAc from substrate proteins, we profiled protein *O*-GlcNAcylation of the two states by mass spectrometry (MS)-based quantitative proteomics. Cell lysates of PXGL naive and primed hESCs were enzymatically tagged with azido-N-acetylgalactosamine (GalNAz) and subsequently derivatized with alkynyl-biotin via the Cu(I)-catalyzed click reaction. Biotinylated O-GlcNAcylated proteins were enriched on streptavidin-coated beads and further subjected to on-beads trypsin digestion to release peptides. The released peptides were subjected to isotopic dimethyl labeling of amino groups by reductive amination and further quantified by MS (Figure 7A). The analysis of all identified proteins revealed that primed hESCs have a higher level of O-GlcNAcylated proteins, consistent with the western blot results (Figures 7B, 1C, 1E, and 1G). Overall, we identified a total of 812 differentially expressed glycoproteins (fold change ≥ 1.5, p value ≤ 0.05, Student's t test), with 69 upregulated and 743 downregulated in naive cells (Figure 7C; Table S4). Kyoto Encyclopedia of Genes and Genomes (KEGG) and Gene Ontology (GO) analyses were performed with the

Figure 5. OGA depletion impacts global gene expressions to regulate pluripotency of hESCs

(A) Schematic depiction of repriming transition of PXGL naive hESCs and the experimental design for RNA-seq.

(B) Volcano plot showing DEGs between WT reprimed and H9 naive hESCs. (fold change ≥ 2, q value ≤ 0.05).

(C) Clustering analysis of RNA-seq data for naive, repriming, and reprimed hESCs with or without OGA depletion based on naive-specific genes (N = 2,809) and reprimed-specific genes (N = 6,382), as defined in Figure 5B.

(D) GSEA analysis in WT and OGA-depleted naive hESCs. Gene sets were considered differentially enriched with p value ≤ 0.05.

(E) Volcano plot showing DEGs between WT and OGA-depleted naive hESCs on day 5 of repriming. (fold change ≥ 2, q value ≤ 0.05).

(F) The number of up- or downregulated DEGs in OGA-depleted versus WT naive, repriming, and reprimed hESCs. (fold change ≥ 2, q value ≤ 0.05).

(G) Venn diagram showing the overlap between DEGs in OGA-depleted versus WT naive, repriming, and reprimed hESCs.

(H) Common clusters of gene sets in OGA-depleted versus WT naive, repriming, and reprimed hESCs. Gene sets with $|NES| \geq 1$, p value ≤ 0.05, or FDR q value ≤ 0.25 were considered.

(I) Heatmap of unique and common DEGs from repriming versus naive cell in shNC or shOGA group and the associated enriched pathways. Venn diagram showing the overlap between DEGs (fold change ≥ 2, q value ≤ 0.05).

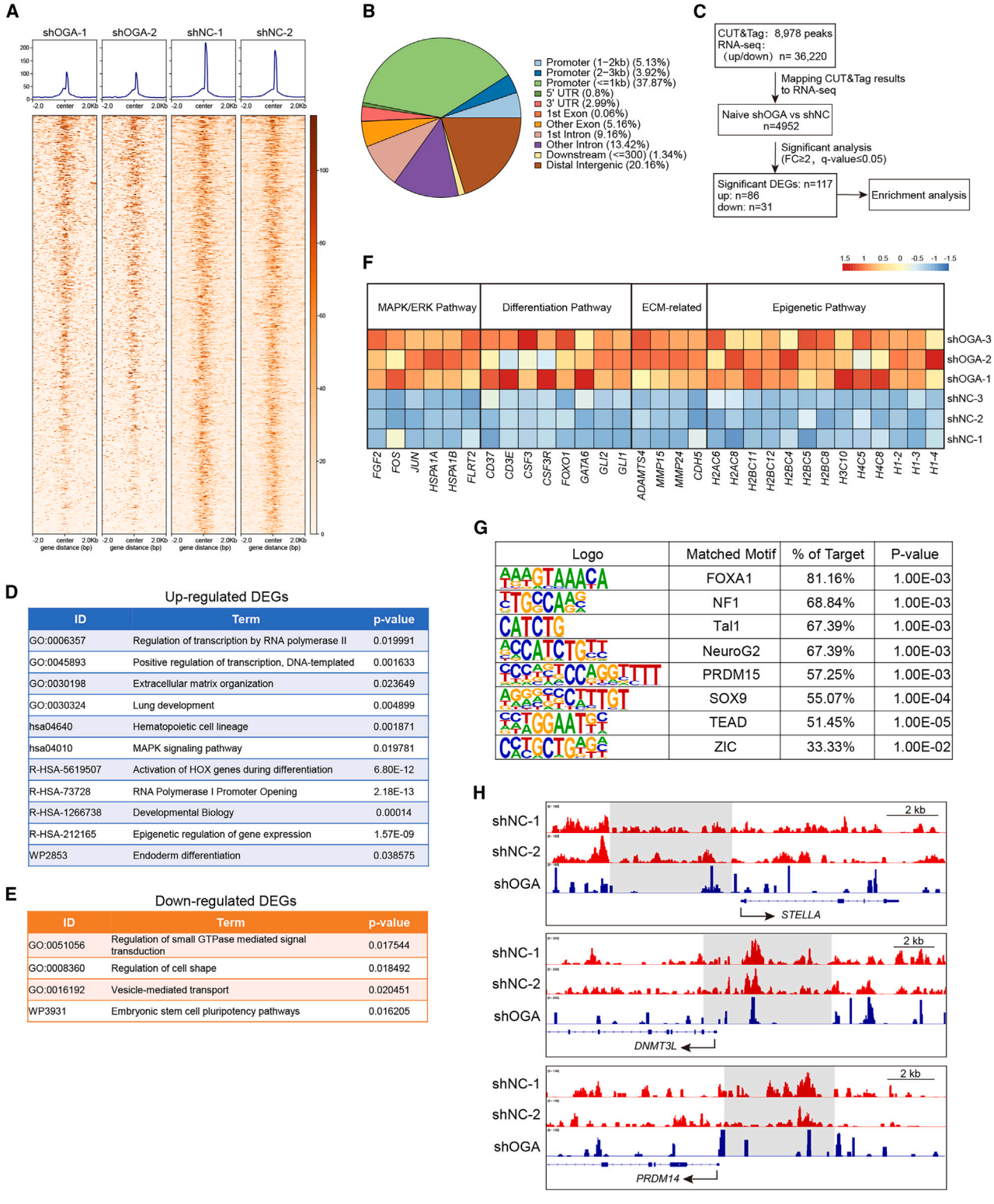

D

Up-regulated DEGs

ID	Term	p-value
GO:0006357	Regulation of transcription by RNA polymerase II	0.019991
GO:0045893	Positive regulation of transcription, DNA-templated	0.001633
GO:0030198	Extracellular matrix organization	0.023649
GO:0030324	Lung development	0.004899
hsa04640	Hematopoietic cell lineage	0.001871
hsa04010	MAPK signaling pathway	0.019781
R-HSA-5619507	Activation of HOX genes during differentiation	6.80E-12
R-HSA-73728	RNA Polymerase I Promoter Opening	2.18E-13
R-HSA-1266738	Developmental Biology	0.00014
R-HSA-212165	Epigenetic regulation of gene expression	1.57E-09
WP2853	Endoderm differentiation	0.038575

E

Down-regulated DEGs

ID	Term	p-value
GO:0051056	Regulation of small GTPase mediated signal transduction	0.017544
GO:0008360	Regulation of cell shape	0.018492
GO:0016192	Vesicle-mediated transport	0.020451
WP3931	Embryonic stem cell pluripotency pathways	0.016205

Figure 6. OGA is involved in transcriptional regulation of stem cell-related genes in hESCs

(A) Average read density and chromatin occupancy heatmaps across the center of OGA binding in OGA-depleted and WT PXGL naive hESCs using CUT&Tag sequencing.

(legend continued on next page)

differentially expressed proteins to investigate which pathways/processes were regulated by O-GlcNAcylation. In the top 20 significantly enriched KEGG pathways are ribosome biogenesis/processing and cell metabolism pathways (Figure 7D). GO analysis of biological processes (BPs) further showed that a large number of proteins (155 out of 812, 19.1% of the total differentially expressed proteins) are involved in cell differentiation and tissue development (Figure 7E). Also, among the differentially expressed *O*-GlcNAcylated proteins, 238 transcription factors/cofactors were identified. These data further support that OGA-mediated O-GlcNAcylation is important for embryonic development and lineage commitment. However, it is still challenging to identify how many or which specific DEGs are regulated due to the change of protein expression or change of *O*-GlcNAc.

DISCUSSION

Accumulating evidence has shown that *O*-GlcNAc plays a pivotal role in regulating the pluripotency of both mESCs and hESCs. In mESCs, upon differentiation OGT decreased and OGA increased, leading to a reduction of *O*-GlcNAc levels (Hao et al., 2023). Both OGA expression and global *O*-GlcNAc level were higher in the primed mESCs compared to the naive state (Miura and Nishihara, 2016). Inhibition of OGT or OGA with inhibitors reduced the transition efficiency from primed mESCs to naive cells (Miura and Nishihara, 2016). Moreover, elevating *O*-GlcNAc through OGA inhibition delayed mESC differentiation but did not affect the transition of naive cells to the primed state (Speakman et al., 2014). Notably, the role of OGT and OGA appears to be quite different in hESCs. Both OGT and OGA expressions were reduced during primed hESCs differentiation (Maury et al., 2013). We show that OGA expression increased and *O*-GlcNAc levels reduced in naive hESCs compared to the primed state. OGA inhibition impaired pluripotency in naive hESCs, but not in primed cells. Consequently, OGA inhibition promoted the transition of naive cells to the primed state, while OGA overexpression promoted the reverse transition. Consistent with previous studies, inhibition of OGT, but not OGA, reduced pluripotency in primed hESCs and accelerated cell differentiation (Andres et al., 2017; Maury et al., 2013). Therefore, OGA and OGT play differential roles in pluripotency regulation between mouse and hESCs. This is not surprising as mESCs and hESCs differ substantially in molecular properties, including signaling pathways, pluripotency marker networks, and cell metabolism (Nichols and Smith, 2009; Van der Jeught et al., 2015; Varzideh et al., 2023). Our study suggests that *O*-GlcNAc regulation may be a key aspect of the human-mouse difference during early embryogenesis. It is also important that modulation of *O*-GlcNAc may improve the efficiency of generating naive hESCs from the conventional primed hESCs *in vitro*.

As *O*-GlcNAc is dynamically controlled by OGT and OGA, it is intriguing to observe that OGT or OGA is differentially required in maintaining pluripotency in different developmental stages of hESCs. In naive hESCs, OGA, but not OGT, plays a role in maintaining pluripotency. Yet in primed hESCs, OGT, instead of OGA, regulates pluripotency. The mechanisms underlying this difference remain to be investigated. We speculate that the expression levels and localization of OGT and OGA isoforms have an important impact. OGT and OGA are likely associated with stage-specific protein complexes (such as chromatin remodelers) to control distinct transcriptional programs in naive and primed hESCs (Hardivillé and Hart, 2016; Myers et al., 2011). Understanding the mechanisms may provide important insights into the complex regulatory network during the pluripotency transition.

O-GlcNAc is important in regulating gene transcription. Both OGT and OGA are shown to localize at gene promoters throughout the genome, with considerable overlaps with RNA polymerase II (Pol II) positions (Resto et al., 2016). In addition, nearly all Pol II transcription factors possess *O*-GlcNAc (Jackson and Tjian, 1988). O-GlcNAcylation of the C-terminal domain (CTD) of Pol II is a prerequisite for the initiation of transcription cycle (Ranuncolo et al., 2012). OGA interacts with the transcription elongation machinery, and OGA-mediated deglycosylation of RNA Pol II precedes the elongation (Chatham et al., 2021; Resto et al., 2016). Furthermore, recycling of *O*-GlcNAc on transcription factors changes their activity, localization, and/or stability, which would further impact the expression of downstream target genes (Chatham et al., 2021). Consistently, we observed that OGA depletion impacts pathways associated with transcription regulation, including RNA Pol II-specific terms (Figure 5H). Subsequent

(B) Distribution of OGA binding peaks across the genome in PXGL naive hESCs.
(C) Schematic of integrative analysis of CUT&Tag and RNA-seq datasets.
(D and E) Enrichment analysis of the upregulated (D) and downregulated (E) OGA-targeted DEGs in OGA-depleted versus WT PXGL naive hESCs.
(F) Heatmap of genes involved in selected pathways and encoded histones.
(G) Motifs enriched at OGA-occupancy sites of DEGs, as determined using HOMER.
(H) Integrative genomics viewer images showing tracks of OGA occupancy on STELLA, DNMT3L, and PRDM14 in PXGL naive hESCs.

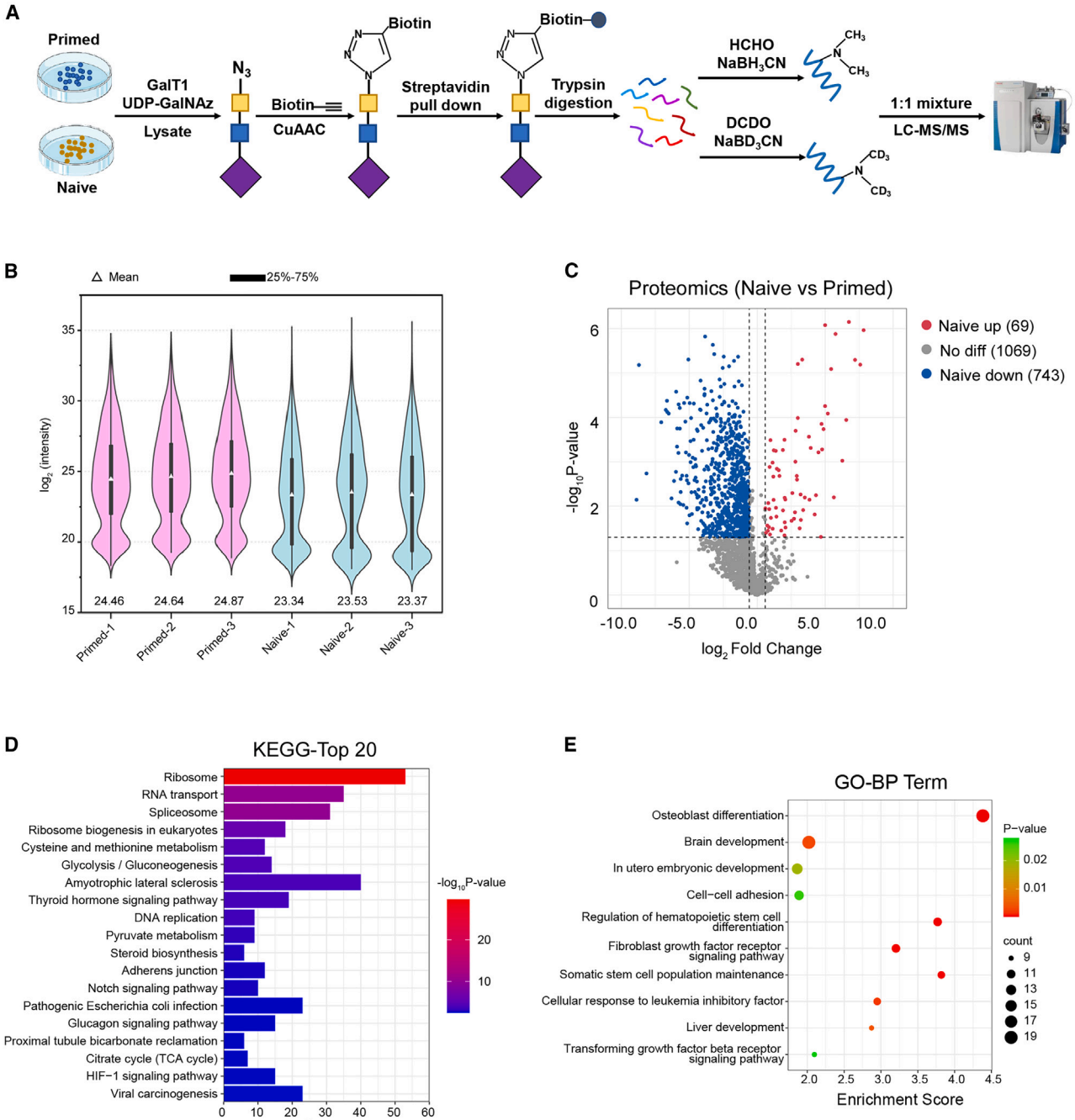

Figure 7. Profiling OGA-mediated protein O-GlcNAcylation during PXGL naive-to-primed transition

(A) Workflow of O-GlcNAcylated proteins enrichment and proteomic analysis.

(B) Violin plots showing the overall characteristics of O-GlcNAcylation level in H9 naive verus primed hESCs.

(C) Volcano plot showing the differentially regulated O-GlcNAcylated proteins between primed and PXGL naive hESCs. (fold change ≥ 1.5, p value ≤ 0.05). "No diff," no significant difference.

(D) KEGG pathway enrichment analysis of the differential O-GlcNAcylated proteins (showing the top 20 hits).

(E) Bubble plot of significantly enriched GO terms (biological process) associated with stem cell properties based on differential O-GlcNAcylated proteins.

CUT&Tag assays and DEGs motif analysis showed that OGA directly regulates transcription factors involved in stem cell pluripotency and differentiation. *O*-GlcNAc is known to respond to cellular nutrient states (Hardivillé and Hart, 2014; 2016) and is a metabolic hub integrating nutrients ranging from glucose, glutamine, and fatty acids, to impact protein structure and function (Akella et al., 2019). The naive and primed hESCs differ drastically in cellular metabolism (Cornacchia et al., 2019; Tsogtbaatar et al., 2020; Zhou et al., 2012). The altered metabolism greatly influences hESCs pluripotency (Cornacchia et al., 2019; Sperber et al., 2015). Thus, *O*-GlcNAc may constitute a key mechanism linking metabolism and the regulation of pluripotency gene expression.

EXPERIMENTAL PROCEDURES

Resource availability

Lead contact

Further information and requests for reagents may be directed to and will be fulfilled by the lead contact, Wen Yi (wyi@zju.edu.cn).

Materials availability

This study did not generate new unique reagents.

Data and code availability

EP300 ChIP-seq data of H1 hESCs (Figure S5E) were derived from the ENCODE database (https://www.encodeproject.org/) (ENCSR000BKK). The RNA-seq or CUT&Tag data generated in this study have been submitted to the NCBI Gene Expression Omnibus (GEO) datasets with accession number GSE228357, GSE256456, GSE260670, and GSE264283.

The O-GlcNAcylated proteins quantitative MS data have been uploaded to the ProteomeXchange Consortium via the PRIDE partner repository (project accession: PXD041605).

Repriming of naive hESCs

The naive-to-primed hESCs transition was performed as previously described, with minor modifications (An et al., 2020; Huang et al., 2021). Naive hESCs were digested into single cells with Accutase (Thermo Fisher, A1110501), and 1×10^5 cells were seeded onto Matrigel/Geltrex (Thermo Fisher, A1413302)-coated six-well plate in the corresponding naive hESCs medium supplemented with 5 μM Y27632 (Selleck, S1049). The next day, media were replaced into mTeSR1 for the following transition. During this period, cells were maintained at 37°C, 5% O_2, 5% CO_2 environment.

All other experimental procedures can be found in the supplemental information.

SUPPLEMENTAL INFORMATION

Supplemental information can be found online at https://doi.org/10.1016/j.stemcr.2024.05.009.

ACKNOWLEDGMENTS

This work was supported by the National Natural Science Foundation of China (NSFC, grant nos. 32271331, 22325704, 92353303 to W.Y.; 32371504, 32088101 to W.Q.) and the Fundamental Research Funds for the Central Universities (K20220228).

AUTHOR CONTRIBUTIONS

W.Y. conceived the project and designed the experiments; Q.L. and C.C. performed cell biology and biochemistry experiments; Z.F. and W.Q. performed mass spectrometry analysis; Q.L., Z.F., H.S.,Y.W., W.Q., and W.Y. analyzed the data; Q.L. and W.Y. wrote the paper with inputs from all authors.

DECLARATION OF INTERESTS

The authors declare no competing interests.

Received: October 13, 2023
Revised: May 26, 2024
Accepted: May 27, 2024
Published: June 27, 2024

REFERENCES

Akella, N.M., Ciraku, L., and Reginato, M.J. (2019). Fueling the fire: emerging role of the hexosamine biosynthetic pathway in cancer. BMC Biol. *17*, 52. https://doi.org/10.1186/s12915-019-0671-3.

An, C., Feng, G., Zhang, J., Cao, S., Wang, Y., Wang, N., Lu, F., Zhou, Q., and Wang, H. (2020). Overcoming Autocrine FGF Signaling-Induced Heterogeneity in Naive Human ESCs Enables Modeling of Random X Chromosome Inactivation. Cell Stem Cell *27*, 482–497.e4. https://doi.org/10.1016/j.stem.2020.06.002.

Andres, L.M., Blong, I.W., Evans, A.C., Rumachik, N.G., Yamaguchi, T., Pham, N.D., Thompson, P., Kohler, J.J., and Bertozzi, C.R. (2017). Chemical Modulation of Protein O-GlcNAcylation via OGT Inhibition Promotes Human Neural Cell Differentiation. ACS Chem. Biol. *12*, 2030–2039. https://doi.org/10.1021/acschembio.7b00232.

Bao, S., Tang, F., Li, X., Hayashi, K., Gillich, A., Lao, K., and Surani, M.A. (2009). Epigenetic reversion of post-implantation epiblast to pluripotent embryonic stem cells. Nature *461*, 1292–1295. https://doi.org/10.1038/nature08534.

Bayerl, J., Ayyash, M., Shani, T., Manor, Y.S., Gafni, O., Massarwa, R., Kalma, Y., Aguilera-Castrejon, A., Zerbib, M., Amir, H., et al. (2021). Principles of signaling pathway modulation for enhancing human naive pluripotency induction. Cell Stem Cell *28*, 1549–1565.e12. https://doi.org/10.1016/j.stem.2021.04.001.

Bredenkamp, N., Stirparo, G.G., Nichols, J., Smith, A., and Guo, G. (2019). The Cell-Surface Marker Sushi Containing Domain 2 Facilitates Establishment of Human Naive Pluripotent Stem Cells. Stem Cell Rep. *12*, 1212–1222. https://doi.org/10.1016/j.stemcr.2019.03.014.

Chatham, J.C., Zhang, J., and Wende, A.R. (2021). Role of O-Linked N-Acetylglucosamine Protein Modification in Cellular (Patho) Physiology. Physiol. Rev. *101*, 427–493. https://doi.org/10.1152/physrev.00043.2019.

Chen, K.G., Johnson, K.R., Park, K., Maric, D., Yang, F., Liu, W.F., Fann, Y.C., Mallon, B.S., and Robey, P.G. (2024). Resistance to Naïve and Formative Pluripotency Conversion in RSeT Human

Embryonic Stem Cells. Preprint at bioRxiv. https://doi.org/10.1101/2024.02.16.580778.

Collier, A.J., and Rugg-Gunn, P.J. (2018). Identifying Human Naïve Pluripotent Stem Cells - Evaluating State-Specific Reporter Lines and Cell-Surface Markers. Bioessays *40*, e1700239. https://doi.org/10.1002/bies.201700239.

Constable, S., Lim, J.M., Vaidyanathan, K., and Wells, L. (2017). O-GlcNAc transferase regulates transcriptional activity of human Oct4. Glycobiology *27*, 927–937. https://doi.org/10.1093/glycob/cwx055.

Cornacchia, D., Zhang, C., Zimmer, B., Chung, S.Y., Fan, Y., Soliman, M.A., Tchieu, J., Chambers, S.M., Shah, H., Paull, D., et al. (2019). Lipid Deprivation Induces a Stable, Naive-to-Primed Intermediate State of Pluripotency in Human PSCs. Cell Stem Cell *25*, 120–136.e10. https://doi.org/10.1016/j.stem.2019.05.001.

Deplus, R., Delatte, B., Schwinn, M.K., Defrance, M., Méndez, J., Murphy, N., Dawson, M.A., Volkmar, M., Putmans, P., Calonne, E., et al. (2013). TET2 and TET3 regulate GlcNAcylation and H3K4 methylation through OGT and SET1/COMPASS. Embo j *32*, 645–655. https://doi.org/10.1038/emboj.2012.357.

Donato, V., Bonora, M., Simoneschi, D., Sartini, D., Kudo, Y., Saraf, A., Florens, L., Washburn, M.P., Stadtfeld, M., Pinton, P., and Pagano, M. (2017). The TDH-GCN5L1-Fbxo15-KBP axis limits mitochondrial biogenesis in mouse embryonic stem cells. Nat. Cell Biol. *19*, 341–351. https://doi.org/10.1038/ncb3491.

Eastham, A.M., Spencer, H., Soncin, F., Ritson, S., Merry, C.L.R., Stern, P.L., and Ward, C.M. (2007). Epithelial-mesenchymal transition events during human embryonic stem cell differentiation. Cancer Res. *67*, 11254–11262. https://doi.org/10.1158/0008-5472.can-07-2253.

Guo, G., von Meyenn, F., Santos, F., Chen, Y., Reik, W., Bertone, P., Smith, A., and Nichols, J. (2016). Naive Pluripotent Stem Cells Derived Directly from Isolated Cells of the Human Inner Cell Mass. Stem Cell Rep. *6*, 437–446. https://doi.org/10.1016/j.stemcr.2016.02.005.

Hanover, J.A., Krause, M.W., and Love, D.C. (2010). The hexosamine signaling pathway: O-GlcNAc cycling in feast or famine. Biochim. Biophys. Acta *1800*, 80–95. https://doi.org/10.1016/j.bbagen.2009.07.017.

Hao, Y., Fan, X., Shi, Y., Zhang, C., Sun, D.E., Qin, K., Qin, W., Zhou, W., and Chen, X. (2019). Next-generation unnatural monosaccharides reveal that ESRRB O-GlcNAcylation regulates pluripotency of mouse embryonic stem cells. Nat. Commun. *10*, 4065. https://doi.org/10.1038/s41467-019-11942-y.

Hao, Y., Li, X., Qin, K., Shi, Y., He, Y., Zhang, C., Cheng, B., Zhang, X., Hu, G., Liang, S., et al. (2023). Chemoproteomic and Transcriptomic Analysis Reveals that O-GlcNAc Regulates Mouse Embryonic Stem Cell Fate through the Pluripotency Network. Angew. Chem. *62*, e202300500. https://doi.org/10.1002/anie.202300500.

Hardivillé, S., and Hart, G.W. (2014). Nutrient regulation of signaling, transcription, and cell physiology by O-GlcNAcylation. Cell Metab. *20*, 208–213. https://doi.org/10.1016/j.cmet.2014.07.014.

Hardivillé, S., and Hart, G.W. (2016). Nutrient regulation of gene expression by O-GlcNAcylation of chromatin. Curr. Opin. Chem. Biol. *33*, 88–94. https://doi.org/10.1016/j.cbpa.2016.06.005.

Hart, G.W., Housley, M.P., and Slawson, C. (2007). Cycling of O-linked beta-N-acetylglucosamine on nucleocytoplasmic proteins. Nature *446*, 1017–1022. https://doi.org/10.1038/nature05815.

Huang, X., Park, K.M., Gontarz, P., Zhang, B., Pan, J., McKenzie, Z., Fischer, L.A., Dong, C., Dietmann, S., Xing, X., et al. (2021). OCT4 cooperates with distinct ATP-dependent chromatin remodelers in naïve and primed pluripotent states in human. Nat. Commun. *12*, 5123. https://doi.org/10.1038/s41467-021-25107-3.

Jackson, S.P., and Tjian, R. (1988). O-glycosylation of eukaryotic transcription factors: implications for mechanisms of transcriptional regulation. Cell *55*, 125–133. https://doi.org/10.1016/0092-8674(88)90015-3.

Keembiyehetty, C., Love, D.C., Harwood, K.R., Gavrilova, O., Comly, M.E., and Hanover, J.A. (2015). Conditional knock-out reveals a requirement for O-linked N-Acetylglucosaminase (O-GlcNAcase) in metabolic homeostasis. J. Biol. Chem. *290*, 7097–7113. https://doi.org/10.1074/jbc.M114.617779.

Lee, H.J., Ryu, J.M., Jung, Y.H., Lee, K.H., Kim, D.I., and Han, H.J. (2016). Glycerol-3-phosphate acyltransferase-1 upregulation by O-GlcNAcylation of Sp1 protects against hypoxia-induced mouse embryonic stem cell apoptosis via mTOR activation. Cell Death Dis. *7*, e2158. https://doi.org/10.1038/cddis.2015.410.

Li, D., Yang, J., Huang, X., Zhou, H., and Wang, J. (2022). eIF4A2 targets developmental potency and histone H3.3 transcripts for translational control of stem cell pluripotency. Sci. Adv. *8*, eabm0478. https://doi.org/10.1126/sciadv.abm0478.

Linneberg-Agerholm, M., Wong, Y.F., Romero Herrera, J.A., Monteiro, R.S., Anderson, K.G.V., and Brickman, J.M. (2019). Naïve human pluripotent stem cells respond to Wnt, Nodal and LIF signalling to produce expandable naïve extra-embryonic endoderm. Development *146*, dev180620. https://doi.org/10.1242/dev.180620.

Love, D.C., Krause, M.W., and Hanover, J.A. (2010). O-GlcNAc cycling: emerging roles in development and epigenetics. Semin. Cell Dev. Biol. *21*, 646–654. https://doi.org/10.1016/j.semcdb.2010.05.001.

Maury, J.J.P., Chan, K.K.K., Zheng, L., Bardor, M., and Choo, A.B.H. (2013). Excess of O-linked N-acetylglucosamine modifies human pluripotent stem cell differentiation. Stem Cell Res. *11*, 926–937. https://doi.org/10.1016/j.scr.2013.06.004.

Maury, J.J.P., El Farran, C.A., Ng, D., Loh, Y.H., Bi, X., Bardor, M., and Choo, A.B.H. (2015). RING1B O-GlcNAcylation regulates gene targeting of polycomb repressive complex 1 in human embryonic stem cells. Stem Cell Res. *15*, 182–189. https://doi.org/10.1016/j.scr.2015.06.007.

McManus, K.J., and Hendzel, M.J. (2003). Quantitative analysis of CBP- and P300-induced histone acetylations in vivo using native chromatin. Mol. Cell Biol. *23*, 7611–7627. https://doi.org/10.1128/mcb.23.21.7611-7627.2003.

Miura, T., and Nishihara, S. (2016). O-GlcNAc is required for the survival of primed pluripotent stem cells and their reversion to the naïve state. Biochem. Biophys. Res. Commun. *480*, 655–661. https://doi.org/10.1016/j.bbrc.2016.10.111.

Myers, S.A., Panning, B., and Burlingame, A.L. (2011). Polycomb repressive complex 2 is necessary for the normal site-specific O-GlcNAc distribution in mouse embryonic stem cells. Proc. Natl. Acad. Sci. USA *108*, 9490–9495. https://doi.org/10.1073/pnas.1019289108.

Myers, S.A., Peddada, S., Chatterjee, N., Friedrich, T., Tomoda, K., Krings, G., Thomas, S., Maynard, J., Broeker, M., Thomson, M., et al. (2016). SOX2 O-GlcNAcylation alters its protein-protein interactions and genomic occupancy to modulate gene expression in pluripotent cells. Elife *5*, e10647. https://doi.org/10.7554/eLife.10647.

Nichols, J., and Smith, A. (2009). Naive and primed pluripotent states. Cell Stem Cell *4*, 487–492. https://doi.org/10.1016/j.stem.2009.05.015.

Pan, C., and Fan, Y. (2016). Role of H1 linker histones in mammalian development and stem cell differentiation. Biochim. Biophys. Acta *1859*, 496–509. https://doi.org/10.1016/j.bbagrm.2015.12.002.

Ranuncolo, S.M., Ghosh, S., Hanover, J.A., Hart, G.W., and Lewis, B.A. (2012). Evidence of the involvement of O-GlcNAc-modified human RNA polymerase II CTD in transcription in vitro and in vivo. J. Biol. Chem. *287*, 23549–23561. https://doi.org/10.1074/jbc.M111.330910.

Resto, M., Kim, B.-H., Fernandez, A.G., Abraham, B.J., Zhao, K., and Lewis, B.A. (2016). O-GlcNAcase Is an RNA Polymerase II Elongation Factor Coupled to Pausing Factors SPT5 and TIF1β. J. Biol. Chem. *291*, 22703–22713. https://doi.org/10.1074/jbc.M116.751420.

Shafi, R., Iyer, S.P., Ellies, L.G., O'Donnell, N., Marek, K.W., Chui, D., Hart, G.W., and Marth, J.D. (2000). The O-GlcNAc transferase gene resides on the X chromosome and is essential for embryonic stem cell viability and mouse ontogeny. Proc. Natl. Acad. Sci. USA *97*, 5735–5739. https://doi.org/10.1073/pnas.100471497.

Singh, J.P., Zhang, K., Wu, J., and Yang, X. (2015). O-GlcNAc signaling in cancer metabolism and epigenetics. Cancer Lett. *356*, 244–250. https://doi.org/10.1016/j.canlet.2014.04.014.

Speakman, C.M., Domke, T.C.E., Wongpaiboonwattana, W., Sanders, K., Mudaliar, M., van Aalten, D.M.F., Barton, G.J., and Stavridis, M.P. (2014). Elevated O-GlcNAc levels activate epigenetically repressed genes and delay mouse ESC differentiation without affecting naïve to primed cell transition. Stem Cell. *32*, 2605–2615. https://doi.org/10.1002/stem.1761.

Sperber, H., Mathieu, J., Wang, Y., Ferreccio, A., Hesson, J., Xu, Z., Fischer, K.A., Devi, A., Detraux, D., Gu, H., et al. (2015). The metabolome regulates the epigenetic landscape during naive-to-primed human embryonic stem cell transition. Nat. Cell Biol. *17*, 1523–1535. https://doi.org/10.1038/ncb3264.

Taei, A., Rasooli, P., Braun, T., Hassani, S.N., and Baharvand, H. (2020). Signal regulators of human naïve pluripotency. Exp. Cell Res. *389*, 111924. https://doi.org/10.1016/j.yexcr.2020.111924.

Takashima, Y., Guo, G., Loos, R., Nichols, J., Ficz, G., Krueger, F., Oxley, D., Santos, F., Clarke, J., Mansfield, W., et al. (2014). Resetting transcription factor control circuitry toward ground-state pluripotency in human. Cell *158*, 1254–1269. https://doi.org/10.1016/j.cell.2014.08.029.

Theunissen, T.W., Powell, B.E., Wang, H., Mitalipova, M., Faddah, D.A., Reddy, J., Fan, Z.P., Maetzel, D., Ganz, K., Shi, L., et al. (2014). Systematic identification of culture conditions for induction and maintenance of naive human pluripotency. Cell Stem Cell *15*, 471–487. https://doi.org/10.1016/j.stem.2014.07.002.

Thompson, J.J., Lee, D.J., Mitra, A., Frail, S., Dale, R.K., and Rocha, P.P. (2022). Extensive co-binding and rapid redistribution of NANOG and GATA6 during emergence of divergent lineages. Nat. Commun. *13*, 4257. https://doi.org/10.1038/s41467-022-31938-5.

Tsogtbaatar, E., Landin, C., Minter-Dykhouse, K., and Folmes, C.D.L. (2020). Energy Metabolism Regulates Stem Cell Pluripotency. Front. Cell Dev. Biol. *8*, 87. https://doi.org/10.3389/fcell.2020.00087.

Van der Jeught, M., Taelman, J., Duggal, G., Ghimire, S., Lierman, S., Chuva de Sousa Lopes, S.M., Deforce, D., Deroo, T., De Sutter, P., and Heindryckx, B. (2015). Application Of Small Molecules Favoring Naïve Pluripotency during Human Embryonic Stem Cell Derivation. Cell. Reprogram. *17*, 170–180. https://doi.org/10.1089/cell.2014.0085.

Varzideh, F., Gambardella, J., Kansakar, U., Jankauskas, S.S., and Santulli, G. (2023). Molecular Mechanisms Underlying Pluripotency and Self-Renewal of Embryonic Stem Cells. Int. J. Mol. Sci. *24*, 8386.

Vella, P., Scelfo, A., Jammula, S., Chiacchiera, F., Williams, K., Cuomo, A., Roberto, A., Christensen, J., Bonaldi, T., Helin, K., and Pasini, D. (2013). Tet proteins connect the O-linked N-acetylglucosamine transferase Ogt to chromatin in embryonic stem cells. Mol. Cell *49*, 645–656. https://doi.org/10.1016/j.molcel.2012.12.019.

Ward, E., Twaroski, K., and Tolar, J. (2017). Feeder-Free Derivation of Naive Human Pluripotent Stem Cells. Stem Cells Dev. *26*, 1087–1089. https://doi.org/10.1089/scd.2017.0067.

Yang, X., and Qian, K. (2017). Protein O-GlcNAcylation: emerging mechanisms and functions. Nat. Rev. Mol. Cell Biol. *18*, 452–465. https://doi.org/10.1038/nrm.2017.22.

Yang, Y.R., Song, M., Lee, H., Jeon, Y., Choi, E.J., Jang, H.J., Moon, H.Y., Byun, H.Y., Kim, E.K., Kim, D.H., et al. (2012). O-GlcNAcase is essential for embryonic development and maintenance of genomic stability. Aging Cell *11*, 439–448. https://doi.org/10.1111/j.1474-9726.2012.00801.x.

Zhou, W., Choi, M., Margineantu, D., Margaretha, L., Hesson, J., Cavanaugh, C., Blau, C.A., Horwitz, M.S., Hockenbery, D., Ware, C., and Ruohola-Baker, H. (2012). HIF1α induced switch from bivalent to exclusively glycolytic metabolism during ESC-to-EpiSC/hESC transition. EMBO J. *31*, 2103–2116. https://doi.org/10.1038/emboj.2012.71.

Zhu, Q., Cheng, X., Cheng, Y., Chen, J., Xu, H., Gao, Y., Duan, X., Ji, J., Li, X., and Yi, W. (2020). O-GlcNAcylation regulates the methionine cycle to promote pluripotency of stem cells. Proc. Natl. Acad. Sci. USA *117*, 7755–7763. https://doi.org/10.1073/pnas.1915582117.